

FIGURE 8. The number of grids with low autofluorescence optical density difference of the 81 grids from the 16 cases of central serous chorioretinopathy. The density was measured by autofluorescence densitometry and spectral-domain optical coherence tomography. There is no significant difference between the acute phase and immediately after resolution in all 16 eyes. In the 5 eyes that were reexamined 3 months after resolution, the number of low autofluorescence optical density difference grids has decreased in Cases 1 and 2. The autofluorescence optical density difference has improved in the 2 eyes. The number of low autofluorescence optical density difference grids has not decreased in the other 3 eyes.

density difference grid did not decrease in the other 3 eyes.

The mean best-corrected VA levels in all cases during the acute phase and immediately after resolution were 0.74 and 0.89, respectively. The mean best-corrected VA level was 1.22 in the 5 eyes 3 months after resolution.

DISCUSSION

IN THE CURRENT STUDY, THE PHOTOPIGMENTS WERE EVALUATED based on the difference in the distribution of the optical density measured by autofluorescence densitometry in eyes with CSC. The area of the SRD had low autofluorescence optical density difference compared to the unaffected area surrounding the SRD. The area of low autofluorescence optical density difference was almost the same size immediately after resolution of the SRD in all eyes. The autofluorescence optical density difference

showed a normal pattern 3 months after resolution of the SRD in 2 eyes. These results suggested that the photopigments decreased in the area of the SRD and did not recover immediately after reattachment.

The VA generally was preserved in CSC despite a retinal detachment. However, many patients with CSC complain of a subjective abnormality in vision such as relative scotoma even after resolution of the SRD. Delayed restoration of the photopigments in CSC has been reported previously.^{14,25} Those results were consistent with our observation. However, analysis of the relation of the visual complaint to the morphologic changes was limited before OCT was introduced. Evaluation of the optical density using FAF makes it feasible to analyze the specific distributions of the photopigments and compare them to the SD-OCT findings. SD-OCT has shown various morphologic changes of the outer retina, such as elongation of the outer segments³ and deposits on the outer retinal surface.^{26,27} The results of autofluorescence densitometry suggested a reduction of the photopigments in

TABLE 1. Profiles of Patients With Central Serous Chorioretinopathy

Patient No.	Age	Gender	Acute Phase					Immediately After Resolution				Three Months After Resolution			
			Duration (Months) ^a	Elongation ^b	fODD	BCVA	LP	Time to Resolution (Months) ^c	IS/OS	fODD	BCVA	After Resolution (Months) ^d	IS/OS	fODD	BCVA
1	47	M	2	Yes	↓	1.0	Yes	3	Irregular	No improvement	1.5	3	Clear	Improvement	1.5
2	32	M	2	Yes	↓	0.5	Yes	3	Irregular	No improvement	1.0	3	Clear	Improvement	1.2
3	49	M	4	Yes	↓	1.2	Yes	5	Irregular	No improvement	1.0	3	Clear	No improvement	1.0
4	37	M	2	Yes	↓	0.9	Yes	4	Irregular	No improvement	0.9	3	Clear	No improvement	1.0
5	56	M	7	No	↓	1.2	Yes	10	Defect	No improvement	1.2	3	Defect	No improvement	1.5
6	49	M	1	Yes	↓	1.2	No	6	Irregular	No improvement	1.2	—	—	—	—
7	61	F	1	Yes	↓	0.7	Yes	4	Irregular	No improvement	1.0	—	—	—	—
8	52	F	1	Yes	↓	1.0	No	8	Irregular	No improvement	1.5	—	—	—	—
9	47	M	3	Yes	↓	1.0	Yes	5	Irregular	No improvement	1.5	—	—	—	—
10	43	M	4	Yes	↓	1.0	No	8	Irregular	No improvement	1.5	—	—	—	—
11	63	M	9	Yes	↓	1.2	Yes	13	Irregular	No improvement	1.2	—	—	—	—
12	48	M	31	Yes	↓	0.9	Yes	32	Irregular	No improvement	1.0	—	—	—	—
13	56	M	61	No	↓	0.4	Yes	64	Defect	No improvement	0.5	—	—	—	—
14	59	M	46	No	↓	0.3	Yes	54	Defect	No improvement	0.2	—	—	—	—
15	31	M	4	No	↓	0.3	No	6	Irregular	No improvement	0.4	—	—	—	—
16	71	M	49	No	↓	0.4	Yes	50	Irregular	No improvement	0.6	—	—	—	—
Mean	50.1		14.2			0.74		17.2			0.89				1.22
SD	11.0		20.3					20.6							

↓ = decreased; BCVA = best-corrected visual acuity; F = female; fODD = autofluorescence optical density difference; IS/OS = photoreceptor inner and outer segment junction; LP = laser photocoagulation; M = male; SD = standard deviation.

^aDuration of symptom from onset.

^bElongation of photoreceptor outer segment.

^cDuration from onset to confirmation of resolution.

^dPeriod from resolution to examination.

the area of the SRD, even though the photoreceptors elongated in the outer retina (Figure 4). The density of the photopigments may decrease in the elongated outer segments. Reduction of the retinal derivatives and related protein as a result of dilution has been presumed to occur in the subretinal space in eyes with CSC.^{14,25} The photoreceptor cells produce the outer segments that contain very few photopigments in the retina of retinoid-deprived rats.²⁸ Engbretson and Witkovsky²⁹ reported that the rod outer segments grow normally in severely vitamin A-deficient *Xenopus* tadpoles. Previous reports and the results of the current study indicate that the photoreceptor cells may continue to produce outer segments that contain few photopigments in eyes with an SRD.

After retinal reattachment, the IS/OS lines on the OCT images were irregular in most eyes with CSC (Table), which suggested 2 possibilities. One is the actual loss of the outer segments, and another is decreased signal intensity attributable to misalignment or disorientation of the outer segments. The Stiles-Crawford effect should be considered in retinal densitometry.¹⁶ However, as orientation of the photoreceptors had little effect on optical density changes measured by FAF,³⁰ autofluorescence densitometry could measure the density of the photopigments despite the fact that the outer segment was not aligned. Therefore, the former possibility is likely. Namely, the disappearance of the IS/OS immediately after resolution in CSC suggests that the outer segments may be phagocytized or absorbed after reattachment, which is consistent with the finding of shortened outer segments after retinal reattachment in experimental retinal detachments.³¹ However, the mechanism of the disappearance of the outer segments is unknown. The renewal rate of the rod outer segments in rat eyes decreased after retinal reattachment because of photoreceptor dysfunction,³² which causes shortening of the outer segment if the shedding of the discs occurs at a normal rate. Impairment of the photoreceptor cells after resolution of SRD in CSC has been proved electrophysiologically.^{11,15} The function of the photoreceptor cells may be involved in the disappearance of the outer segments.

Long-standing macular dysfunction has been reported in recent clinical or electrophysiologic studies.^{8,10,12,33} Delayed restoration of the photopigments may contribute to macular dysfunction because vitamin A deprivation impairs retinal sensitivity.^{34,35} However, the relationship between the density of the photopigments and retinal sensitivity is not seen clearly in eyes with CSC. Further studies are needed to understand this. Photoreceptor apoptosis should be considered to investigate visual function in CSC, since apoptosis has been reported in experimental retinal detachment and human retinal detachment within a few days.^{31,36,37}

Eyes with an irregular IS/OS immediately after resolution of a SRD had fewer photopigments corresponding to the area of the irregular IS/OS on the autofluorescence optical density difference map. Two of the 5 eyes that recovered a clearly delineated IS/OS had a normal auto-

fluorescence optical density difference distribution 3 months after resolution of the SRD. The findings of the IS/OS on OCT images corresponded to the status of the photopigments measured by autofluorescence densitometry. However, the autofluorescence optical density difference and the % autofluorescence optical density difference did not improve in 2 eyes with a clearly delineated IS/OS 3 months after resolution of the SRD (Figure 6), suggesting that a well-delineated IS/OS line indicates photopigment formation but does not assure a normal concentration of photopigments in the outer segments. This result may reflect relative scotoma after resolution of SRD. Since the outer segment discs were synthesized in vitamin A-deprived animals,^{28,38} few photopigments containing outer segments may be produced in human eyes. Since a reduction of the photopigments in eyes without pathologic changes in aged individuals has been reported,^{39,40} photopigments may decrease in aged persons with normal IS/OS findings. Further studies are needed.

The current study had several weaknesses, including a small number of cases and short follow-up time. It is difficult to evaluate the absolute value of the density of the photopigments, because HRA2 does not have apparatus to determine the laser intensity to expose photopigments and the rate of attenuation of autofluorescence from the fundus. As a result, the autofluorescence optical density difference could not be compared directly among the cases. Since the autofluorescence densitometry in our technique primarily measures the rod photopigments, the data are unsuitable for assessing the photopigments at the fovea. With regard to the light absorbance characteristics, autofluorescence optical density difference may be affected by macular pigments and cone photopigments. Because of absorption by the macular pigment, the AF signal is low at the fovea. Therefore no differences of AF intensity can be observed between bleached and unbleached state. We could observe the decline of photopigments and related functional impairment in the area of SRD except for the fovea. Although most subjective vision complaints are about central vision, abnormalities of parafoveal and perifoveal function, which can be detected by our technique, also affect subjective symptoms. These problems may be overcome by using a longer light source for the measurements. On the other hand, recent research reported that quantitative measurement of FAF can be performed with HRA2 modified by insertion of a fluorescence reference chip (Duncker T, et al. IOVS 2010;51:ARVO E-Abstract 262). Quantitative measurement of photopigment might be achieved using this method in combination with autofluorescence densitometry.

In conclusion, we observed reduction and recovery of photopigments in CSC under different conditions. We think that autofluorescence densitometry can evaluate retinal function based on the changes in the photopigments in CSC figures 3 and 5.

THE AUTHORS INDICATE NO FINANCIAL SUPPORT OR NO FINANCIAL CONFLICT OF INTEREST. INVOLVED IN DESIGN AND conduct of study (A.O., T.I., T.S.); collection (A.O., I.M., Y.S.), management, analysis, and interpretation of data (A.O., T.I., T.S., I.M.); and preparation and review (A.O., T.I.) and approval of the manuscript (A.O., T.I., T.S., I.M., Y.S.). This study followed the tenets of the Declaration of Helsinki. The institutional review board at Fukushima Medical University School of Medicine approved: 1) observation using OCT and autofluorescence densitometry for eyes with macular and retinal disorder; 2) the observational study for CSC and its similar disorders at the treatment and follow-up; and 3) the prospective comparative analysis performed in this study.

REFERENCES

1. Maruko I, Iida T, Sekiryu T, Saito M. Morphologic changes in the outer layer of the detached retina in rhegmatogenous retinal detachment and central serous chorioretinopathy. *Am J Ophthalmol* 2009;147(3):489–494 e1.
2. Piccolino FC, de la Longrais RR, Ravera G, et al. The foveal photoreceptor layer and visual acuity loss in central serous chorioretinopathy. *Am J Ophthalmol* 2005;139(1):87–99.
3. Matsumoto H, Kishi S, Otani T, Sato T. Elongation of photoreceptor outer segment in central serous chorioretinopathy. *Am J Ophthalmol* 2008;145(1):162–168.
4. Ojima Y, Hangai M, Sasahara M, et al. Three-dimensional imaging of the foveal photoreceptor layer in central serous chorioretinopathy using high-speed optical coherence tomography. *Ophthalmology* 2007;114(12):2197–2207.
5. Iida T, Hagimura N, Sato T, Kishi S. Evaluation of central serous chorioretinopathy with optical coherence tomography. *Am J Ophthalmol* 2000;129(1):16–20.
6. Furuta M, Iida T, Kishi S. Foveal thickness can predict visual outcome in patients with persistent central serous chorioretinopathy. *Ophthalmologica* 2009;223(1):28–31.
7. Iida T, Yannuzzi LA, Spaide RF, Borodoker N, Carvalho CA, Negrao S. Cystoid macular degeneration in chronic central serous chorioretinopathy. *Retina* 2003;23(1):1–7; quiz 137–138.
8. Matsumoto H, Sato T, Kishi S. Outer nuclear layer thickness at the fovea determines visual outcomes in resolved central serous chorioretinopathy. *Am J Ophthalmol* 2009;148(1):105–110 e1.
9. Ozdemir H, Karacorlu SA, Senturk F, Karacorlu M, Uysal O. Assessment of macular function by microperimetry in unilateral resolved central serous chorioretinopathy. *Eye (Lond)* 2008;22(2):204–208.
10. Ojima Y, Tsujikawa A, Hangai M, et al. Retinal sensitivity measured with the micro perimeter 1 after resolution of central serous chorioretinopathy. *Am J Ophthalmol* 2008;146(1):77–84.
11. Vajaranant TS, Szlyk JP, Fishman GA, Gieser JP, Seiple W. Localized retinal dysfunction in central serous chorioretinopathy as measured using the multifocal electroretinogram. *Ophthalmology* 2002;109(7):1243–1250.
12. Suzuki K, Hasegawa S, Usui T, et al. Multifocal electroretinogram in central serous chorioretinopathy. *Jpn J Ophthalmol* 2000;44(5):571.
13. Theelen T, Berendschot TT, Boon CJ, Hoyng CB, Klevering BJ. Analysis of visual pigment by fundus autofluorescence. *Exp Eye Res* 2008;86(2):296–304.
14. van Meel GJ, Smith VC, Pokorny J, van Norren D. Foveal densitometry in central serous choroidopathy. *Am J Ophthalmol* 1984;98(3):359–368.
15. Miyake Y, Shiroyama N, Ota I, Horiguchi M. Local macular electroretinographic responses in idiopathic central serous chorioretinopathy. *Am J Ophthalmol* 1988;106(5):546–550.
16. DeLint PJ, Berendschot TT, van Norren D. A comparison of the optical Stiles-Crawford effect and retinal densitometry in a clinical setting. *Invest Ophthalmol Vis Sci* 1998;39(8):1519–1523.
17. Alpern M, Pugh EN Jr. The density and photosensitivity of human rhodopsin in the living retina. *J Physiol* 1974;237(2):341–370.
18. Rushton WA, Campbell FW. Measurement of rhodopsin in the living human eye. *Nature* 1954;174(4441):1096–1097.
19. van Norren D, van der Kraats J. A continuously recording retinal densitometer. *Vision Res* 1981;21(6):897–905.
20. Liem AT, Keunen JE, van Norren D, van de Kraats J. Rod densitometry in the aging human eye. *Invest Ophthalmol Vis Sci* 1991;32(10):2676–2682.
21. Tornow RP, Stilling R, Zrenner E. Scanning laser densitometry and color perimetry demonstrate reduced photopigment density and sensitivity in two patients with retinal degeneration. *Vision Res* 1999;39(21):3630–3641.
22. Burns SA, Eisner AE, Lobes LA Jr. Foveal cone photopigment bleaching in central serous retinopathy. *Appl Opt* 1988;27(6):1045–1049.
23. Liem AT, Keunen JE, Van Norren D. Clinical applications of fundus reflection densitometry. *Surv Ophthalmol* 1996;41(1):37–50.
24. Sekiryu T, Iida T, Maruko I, Horiguchi M. Clinical application of autofluorescence densitometry using a scanning laser ophthalmoscope. *Invest Ophthalmol Vis Sci* 2009;50(6):2994–3002.
25. Chuang EL, Sharp DM, Fitzke FW, Kemp CM, Holden AL, Bird AC. Retinal dysfunction in central serous retinopathy. *Eye* 1987;1(Pt 1):120–125.
26. Spaide RF, Klancnik JM Jr. Fundus autofluorescence and central serous chorioretinopathy. *Ophthalmology* 2005;112(5):825–833.
27. Kon Y, Iida T, Maruko I, Saito M. The optical coherence tomography-ophthalmoscope for examination of central serous chorioretinopathy with precipitates. *Retina* 2008;28(6):864–869.
28. Katz ML, Kutryb MJ, Norberg M, Gao CL, White RH, Stark WS. Maintenance of opsin density in photoreceptor outer segments of retinoid-deprived rats. *Invest Ophthalmol Vis Sci* 1991;32(7):1968–1980.
29. Engbretson GA, Witkovsky P. Rod sensitivity and visual pigment concentration in *Xenopus*. *J Gen Physiol* 1978;72(6):801–819.
30. Prieto PM, McLellan JS, Burns SA. Investigating the light absorption in a single pass through the photoreceptor layer by means of the lipofuscin fluorescence. *Vision Res* 2005;45(15):1957–1965.

31. Lewis GP, Charteris DG, Sethi CS, Leitner WP, Linberg KA, Fisher SK. The ability of rapid retinal reattachment to stop or reverse the cellular and molecular events initiated by detachment. *Invest Ophthalmol Vis Sci* 2002;43(7):2412-2420.
32. Guerin CJ, Lewis GP, Fisher SK, Anderson DH. Recovery of photoreceptor outer segment length and analysis of membrane assembly rates in regenerating primate photoreceptor outer segments. *Invest Ophthalmol Vis Sci* 1993;34(1):175-183.
33. Baran NV, Gurlu VP, Esgin H. Long-term macular function in eyes with central serous chorioretinopathy. *Clin Experiment Ophthalmol* 2005;33(4):369-372.
34. Kemp CM, Jacobson SG, Borruat FX, Chaitin MH. Rhodopsin levels and retinal function in cats during recovery from vitamin A deficiency. *Exp Eye Res* 1989;49(1):49-65.
35. Kemp CM, Jacobson SG, Faulkner DJ, Walt RW. Visual function and rhodopsin levels in humans with vitamin A deficiency. *Exp Eye Res* 1988;46(2):185-197.
36. Cook B, Lewis GP, Fisher SK, Adler R. Apoptotic photoreceptor degeneration in experimental retinal detachment. *Invest Ophthalmol Vis Sci* 1995;36(6):990-996.
37. Arroyo JG, Yang L, Bula D, Chen DF. Photoreceptor apoptosis in human retinal detachment. *Am J Ophthalmol* 2005;139(4):605-610.
38. Herron WL Jr, Riegel BW. Production rate and removal of rod outer segment material in vitamin A deficiency. *Invest Ophthalmol* 1974;13(1):46-53.
39. Curcio CA, Millican CL, Allen KA, Kalina RE. Aging of the human photoreceptor mosaic: evidence for selective vulnerability of rods in central retina. *Invest Ophthalmol Vis Sci* 1993;34(12):3278-3296.
40. Elsner AE, Burns SA, Beausencourt E, Weiter JJ. Foveal cone photopigment distribution: small alterations associated with macular pigment distribution. *Invest Ophthalmol Vis Sci* 1998;39(12):2394-2404.

SUBFOVEAL CHOROIDAL THICKNESS AFTER TREATMENT OF VOGT-KOYANAGI-HARADA DISEASE

ICHIRO MARUKO, MD,* TOMOHIRO IIDA, MD,* YUKINORI SUGANO, MD,* HIROSHI OYAMADA, MD,* TETSUJU SEKIRYU, MD,* TAKAMITSU FUJIWARA, MD,† RICHARD F. SPAIDE, MD‡

Purpose: To evaluate the subfoveal choroidal thickness in Vogt-Koyanagi-Harada (VKH) disease using enhanced depth imaging optical coherence tomography.

Methods: Retrospective observational study. Subfoveal choroidal thickness was measured using enhanced depth imaging optical coherence tomography, in which the optical coherence tomography instrument was placed close enough to the eye to obtain an inverted image, which was averaged for 100 scans. All patients were diagnosed as having the ocular findings of VKH disease with or without extraocular disorders. The patients were followed during their initial treatment with corticosteroids.

Results: All 8 patients (16 eyes) with acute phase VKH disease presented with thickening of the choroid. The serous retinal detachment disappeared in 1 month after corticosteroid treatment. The mean choroidal thickness in 16 eyes decreased from $805 \pm 173 \mu\text{m}$ at the first visit to $524 \pm 151 \mu\text{m}$ at 3 days ($P < 0.001$) and $341 \pm 70 \mu\text{m}$ by 2 weeks ($P < 0.001$).

Conclusion: Patients with active VKH disease have markedly thickened choroids, possibly related not only to inflammatory infiltration but also to increased exudation. Both the choroidal thickness and the exudative retinal detachment decreased quickly with corticosteroid treatment. Enhanced depth imaging optical coherence tomography can be used to evaluate the choroidal involvement in VKH disease in the acute stages and may prove useful in the diagnosis and management of this disease noninvasively.

RETINA 31:510-517, 2011

Vogt-Koyanagi-Harada (VKH) disease is a bilateral granulomatous uveitis characterized by the iridocyclitis and exudative retinal detachment in the acute stage. Although the extraocular manifestations in VKH disease are also reported such as meningismus, tinnitus, perception deafness, cerebrospinal fluid pleocytosis, alopecia, poliosis of the eyebrow, eyelashes and scalp hair, and depigmentation of

skin,^{1,2} some patients with only ocular findings are diagnosed as probable or incomplete VKH disease according to its criteria.

Ocular findings of VKH disease, including probable and incomplete cases,² show the following characteristics independent of any extraocular disorders: in the acute stage, fluorescein angiography shows multifocal leaks from the level of retinal pigment epithelium (RPE) with later multilobular pooling of dye within multiple serous retinal detachments. Indocyanine green angiography shows patchy filling delays and blockage by subretinal fluid with hypofluorescent spots with interspersed areas of increased fluorescence and indistinct visualization of choroidal vessels, which are often seen throughout all phases, and there can be late segmental staining of choroidal vessels.³⁻⁷ Optical coherence tomography (OCT) shows partitioned subretinal fluid with associated intraretinal edema.⁸⁻¹¹ In the chronic

From the *Department of Ophthalmology, School of Medicine, Fukushima Medical University, Fukushima, Japan; †Department of Ophthalmology, School of Medicine, Iwate Medical University, Morioka, Japan; and ‡Vitreous Retina Macula Consultants of New York, New York, New York.

The authors have no proprietary or commercial interest in any materials discussed in this article.

Reprint requests: Ichiro Maruko, MD, Department of Ophthalmology, School of Medicine, Fukushima Medical University, 1 Hikarigaoka, Fukushima, 960-1295, Japan; e-mail: imaruko@fmu.ac.jp

and remission stage, a sunset glow fundus, peripheral atrophy, and scarring of the RPE are observed.

Vogt-Koyanagi-Harada disease is a common form of uveitis in Asia, especially in Japan.^{1,2,12,13} Vogt-Koyanagi-Harada disease appears to originate from the choroid. Evaluating the choroidal involvement has potential importance for assessing treatment efficacy and recurrence in VKH disease. Indocyanine green angiography enables visualization of the choroidal vessels; however, it limited the utility for VKH disease because diagnostic characteristics include the blurred visualization of choroid. Also, indocyanine green angiography is invasive and inconvenient to perform repeatedly during the course of a patient's follow-up. B-mode ultrasonographic imaging is capable of demonstrating more marked amounts of choroidal thickening^{14,15}; however, the resolution of conventional ultrasonography is orders of magnitude less than that of OCT. Recently, a new method for the evaluation of the choroid was developed and called enhanced depth imaging OCT (EDI-OCT).¹⁶ In the current study, we observed the morphologic choroidal change during the treatment in the acute stage of ocular finding of VKH disease using EDI-OCT.

Methods

This retrospective study followed the tenets of the Declaration of Helsinki. The Institutional Review Board at the Fukushima Medical University School of Medicine and the Iwate Medical University approved the observation and the retrospective comparative analysis using OCT for eyes with macular and retinal disorders.

Each patient had a complete ophthalmic examination to include indirect ophthalmoscopy, slit-lamp biomicroscopy with a contact lens, and digital fluorescein and indocyanine green angiography (TRC-50IX/IMAGEnet H1024 system; Topcon, Tokyo, Japan). The patients had best-corrected visual acuity measurements that were obtained with a Japanese standard decimal visual chart and calculated by logarithm of the minimum angle of resolution scale for comparing the mean best-corrected visual acuity. All eyes were examined by the Heidelberg Spectralis OCT (Heidelberg Engineering, Heidelberg, Germany) with eye tracking and image averaging systems. The vertical and horizontal scans were obtained at each measurement to evaluate the center of fovea precisely. Follow-up function with Spectralis OCT software was used to avoid measuring the different position with first examination.

Table 1. The Clinical Changes of Choroidal Thickness and Height of Serous Retinal Detachment During the Follow-up Periods in VKH Disease

Patient	Age	Gender*	Diag- nosis	Mening- ismus	Auditory Findings	Integu- mentary	Eye Type	Choroidal Thickness (μm)							Height of SRD (μm)						
								Baseline	Day 1	Day 3	Day 7	Day 14	Baseline	Day 1	Day 3	Day 7	Day 14				
1	30	M	Incomplete	Yes	Deafness	None	OD SRD	1,000†	721	695	499	341	647	209	194	143	0				
							OS SRD	1,000†	1,000†	890	543	355	1,234	146	186	119	0				
2	54	M	Incomplete	Yes	Deafness	None	OD SRD	872	782	639	452	318	115	184	173	194	86				
							OS SRD	843	720	626	428	325	165	177	81	104	57				
3	41	F	Incomplete	Yes	Deafness	None	OD SRD	612	568	—	415	413	786	616	—	102	24				
							OS SRD	576	555	—	484	392	522	247	—	57	0				
4	17	F	Incomplete	Yes	Tinnitus	None	OD SRD	656	577	412	319	266	345	150	131	126	0				
							OS Papillitis	570	440	308	259	233	0	0	0	0	0				
5	51	F	Incomplete	Yes	Tinnitus	None	OD SRD	955	805	509	421	396	208	188	186	87	0				
							OS SRD	963	774	451	404	371	263	210	163	112	0				
6	22	F	Incomplete	Yes	None	None	OD SRD	1,000†	975	762	569	465	847	825	529	213	0				
							OS SRD	1,000†	930	627	531	443	776	689	324	101	0				
7	41	M	Incomplete	NA	Tinnitus	None	OD SRD	681	571	445	335	306	72	74	59	30	0				
							OS SRD	876	688	523	405	328	163	187	133	72	0				
8	35	F	Probable	NA	None	None	OD SRD	649	550	339	278	261	189	134	72	44	0				
							OS SRD	634	461	311	250	245	200	172	50	0	0				
Mean ± SD	36.4	—	—	—	—	—	—	805 ± 173	695 ± 175	524 ± 151	412 ± 101	341 ± 70	408 ± 352	263 ± 232	163 ± 133	94 ± 60	10				
																		25			

Choroidal thickness measured using the spectral-domain EDI-OCT technique.

*Male to female ratio was 3:5.

†These are defined as a 1,000 μm because the inner scleral border cannot be visualized when choroidal thickness values become more than 1,000 μm. NA, not available; Deafness, perceptive deafness; SRD, serous retinal detachment type of VKH disease; Papillitis, papillitis type of VKH disease.

The diagnosis of VKH disease was based on the appearance of bilateral uveitis associated with exudative retinal detachment. In all patients, secondary multiple leaks from the level of the RPE were seen during fluorescein angiography. The patients had no history of trauma or surgery. We ruled out the patients with lymphoma and other forms of uveitis. All patients were diagnosed as having the ocular findings of VKH disease with or without extraocular disorders. At the same time, we also diagnosed the patients according to the diagnostic criteria for VKH disease.² The diagnosis of complete VKH disease mandates the presence of neurologic and auditory findings and the integumentary signs. In case of no presence of the neurologic, auditory, or integumentary signs, we diagnosed probable VKH disease. In case of the presence of any of them, we diagnosed incomplete VKH disease.

The choroid was imaged by positioning the Heidelberg Spectralis instrument close enough to the eye to obtain an inverted image. The OCT instrument was centered on the eye such that the posterior pole image was not tilted. Each image was the product of 100 averaged scans. Using the software (version 1.5.12.0) with Heidelberg Spectralis OCT, the choroid was measured from the outer border of the hyper-reflective line corresponding to the RPE to the inner scleral border. The subfoveal choroidal thickness in both vertical and horizontal sections ($30^\circ \times 30^\circ$) through the center of the fovea was measured, and the average of the 2 was recorded. When choroidal thickness values become more than $1,000 \mu\text{m}$, these are defined as a $1,000 \mu\text{m}$ because the inner scleral border could not be visualized by EDI-OCT. The height of retinal detachment at the fovea was also measured at the same time. The height of retinal detachment was defined as the distance between the outer surface of the neurosensory retina and the inner surface of the RPE. The reported measurements from OCT images represented the average of the horizontal and vertical measurements made by three co-authors (I.M., Y.S., and H.O.) who were masked to the treatment status. The results of the measurement of the choroidal thickness and the height of retinal detachment were analyzed using the Wilcoxon signed rank test.

Results

Sixteen eyes of 8 patients (3 men and 5 women; mean age, 36.4 years) with acute phase of VKH disease were evaluated. All patients visited within 1 month from the subjective onset during April and October in 2009. None of the patients had a history of

either penetrating ocular trauma or surgery and all presented with subjective vision loss, headache, and mild fever. Six patients had meningismus with cerebrospinal fluid pleocytosis (Two additional cases of meningismus refused lumbar puncture.). Three patients had the perceptible hearing loss and another three patients had tinnitus. No cases showed any integumentary signs or any abnormality in their laboratory evaluation including the chest roentgenogram or serum angiotensin-converting enzyme levels. No eyes showed hyperemia of the conjunctiva, microphthalmia, and scleral thickening. Fifteen eyes had serous retinal detachment involving the fovea and multiple focal leaks at the level of RPE during fluorescein angiography. The remaining left eye of Patient 4 showed optic disk hyperemia and foveal striate secondary to papillitis without actual retinal detachment. All 16 eyes showed the leakage from the optic nerve head during fluorescein angiography, and patchy filling delay with indistinct choroidal vessels in indocyanine green angiography. We diagnosed all 8 cases as having the ocular findings of VKH disease

Choroidal Thickness at Baseline and Following Treatment

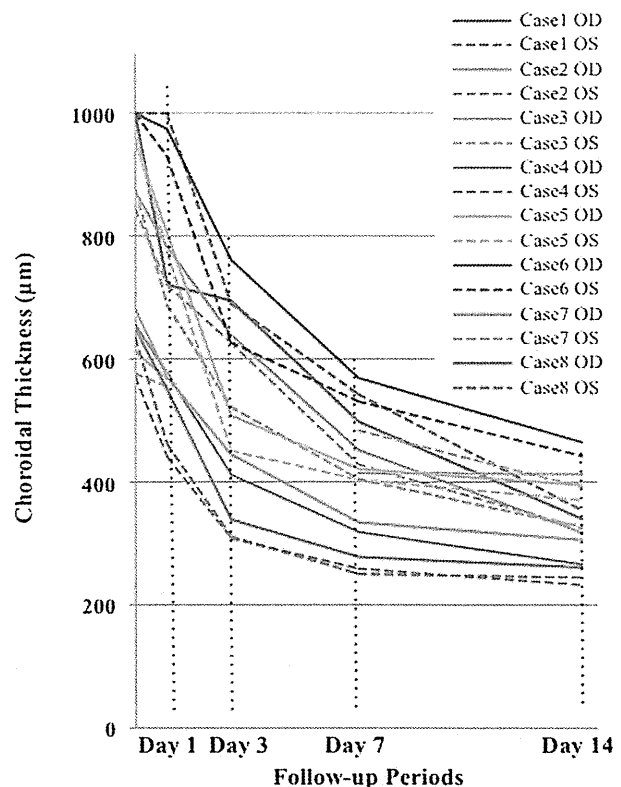


Fig. 1. The changes of the choroidal thickness in all 16 eyes during the follow-up periods. The mean choroidal thickness decreased from baseline to 86% at Day 1, 65% at Day 3, 51% at Day 7, and 42% at Day 14 of its original value.

(7 cases diagnosed as incomplete VKH and 1 case diagnosed as probable VKH). The left eye of Patient 4 was diagnosed as having the papillitis form of VKH disease. After the diagnosis, the patients were given 1,000 mg of intravenous methylprednisolone for 3 days followed by low-dose intravenous betamethasone or oral prednisolone or both.

The clinical changes of the choroidal thickness during the follow-up periods in all cases were summarized in Table 1 and Figure 1. Day 1, Day 3, and Day 14 were defined by the time intervals after initiation of the intravenous therapy. In both eyes of Patient 3, the choroidal thickness at Day 3 was not obtained. The serous retinal detachment resolved in 12 eyes by Day 14 and in all eyes by 1 month. The mean decimal BCVA levels improved from 0.71 (20/28) (0.15 logMAR) at baseline to 1.04 (20/19) (−0.02 logMAR) after resolution of serous retinal detachment ($P < 0.001$). Figures 2 and 3 were illustrated as the representative case with the ocular findings of VKH

disease, and Figures 4 and 5 were illustrated as the representative case with the papillitis type of VKH disease.

The mean choroidal thickness in 16 eyes at baseline was $805 \pm 173 \mu\text{m}$, which decreased to $695 \pm 175 \mu\text{m}$ at Day 1 ($P < 0.001$), $524 \pm 151 \mu\text{m}$ by Day 3 ($P < 0.001$), and $341 \pm 70 \mu\text{m}$ at Day 14 ($P < 0.001$). Choroidal thickness decreased during the course of treatment in all eyes. This corresponds to a percentage reduction from baseline of 14% at Day 1, 35% at Day 3, 49% at Day 7, and 58% at Day 14. The height of retinal detachment decreased from $408 \pm 352 \mu\text{m}$ at baseline to $163 \pm 133 \mu\text{m}$ at Day 3 ($P = 0.003$) and $10 \pm 25 \mu\text{m}$ at Day 14 ($P < 0.001$), respectively.

Discussion

The choroidal thickness in patients with active onset VKH disease was much thicker than that reported for normal eyes¹⁷ and the thickness dramatically

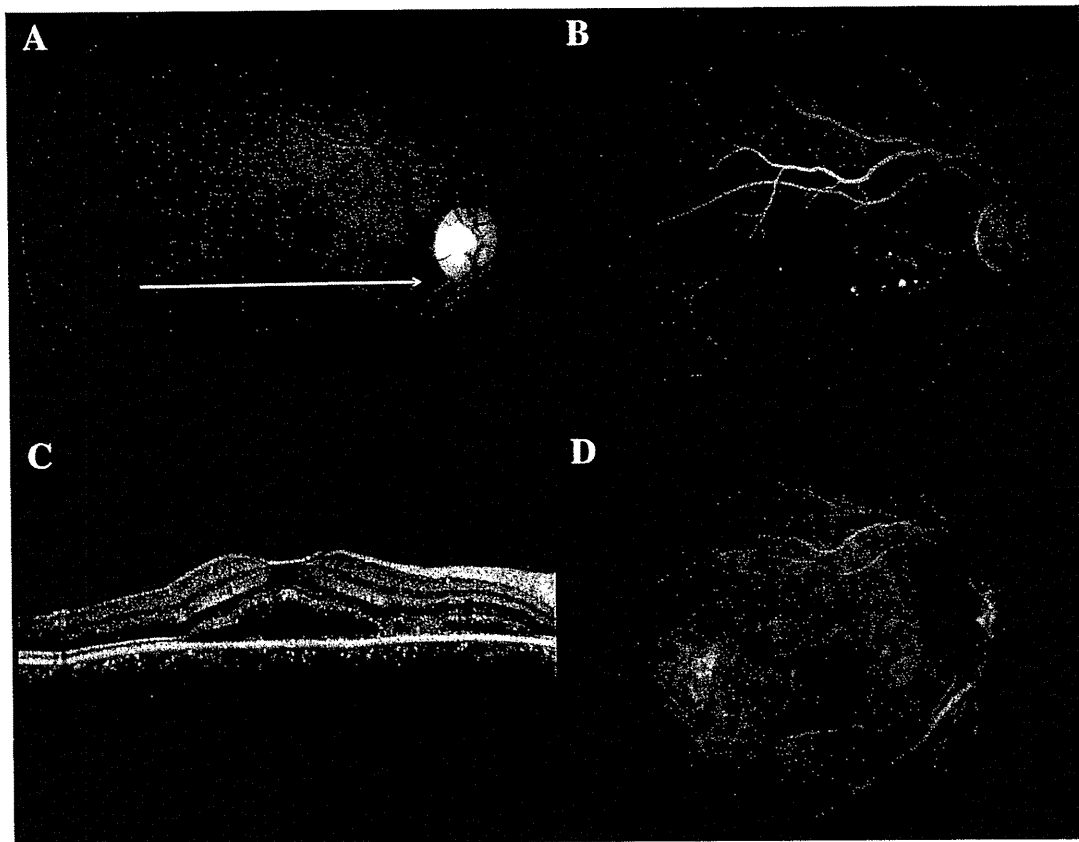


Fig. 2. Patient 8. A 35-year-old woman complained of decreased vision in both eyes for 2 weeks before presentation. The best-corrected visual acuity at baseline was 0.7 (20/29) (0.15 logMAR) in the right eye. **A.** Red-free fundus photography in the right eye showed a serous retinal detachment at baseline. **B.** Fluorescein angiography in the right eye showed multiple focal leaks and hyperfluorescence because of pooling in the subretinal space at baseline. **C.** Spectral-domain OCT in the right eye showed the serous retinal detachment of the macula and nasal to the macula. Spectral-domain OCT in the right eye (white arrow in fundus photograph) showed the serous retinal detachment of the macula and nasal to the macula. **D.** Indocyanine green angiography in the right eye showed patchy filling defects and the indistinct visualization of the choroidal vessels at baseline. She was diagnosed as having VKH disease. She was given intravenous methylprednisolone (1,000 mg, for 3 days) followed by tapered oral prednisolone starting at 40 mg/day.

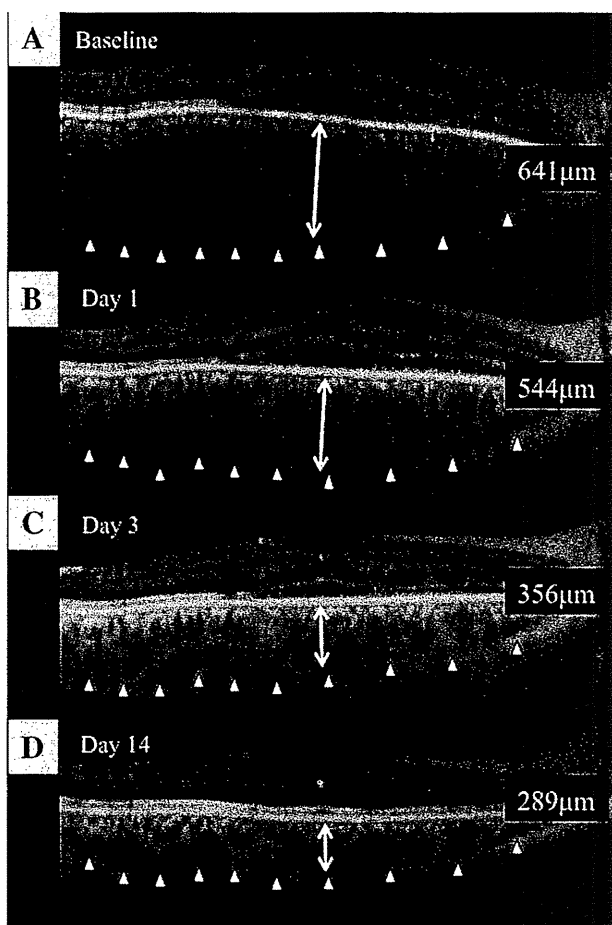


Fig. 3. Enhanced depth imaging spectral-domain OCT images of Patient 8. All images obtained using the technique described in this article are inverted. **A.** The choroidal thickness in the right eye under the fovea from the horizontal scan is $641\ \mu\text{m}$ at baseline. The height of retinal detachment in the right eye under the fovea from the horizontal scan was $189\ \mu\text{m}$. The choroidal thickness in the right eye decreased to $544\ \mu\text{m}$ at Day 1 (**B**), $356\ \mu\text{m}$ at Day 3 (**C**), and $289\ \mu\text{m}$ at Day 14 (**D**) after corticosteroid treatment. Resolution of the retinal detachment is observed at Day 14. The best-corrected visual acuity on Day 14 was 0.8 (20/25) (0.10 logMAR) in the right eye.

decreased after corticosteroid treatment. The serous retinal detachment decreased concurrently. By 1 month after initiation of corticosteroid treatment, the choroidal thickness was normal and the serous retinal detachment resolved.

Vogt-Koyanagi-Harada disease is a multisystem disorder that causes a bilateral granulomatous panuveitis. Affected patients have hyperemia of the optic nerve head and exudative retinal detachments.^{1,2,12,13} Patchy filling delay with hypofluorescent spots and indistinct visualization of the choroidal vessels during indocyanine green angiography are hallmarks of the disease.³⁻⁷ Improvement in the indocyanine green angiographic findings can be seen with treatment, although there are residual effects, such as patchy

filling that remain. B-mode ultrasound imaging is also one of the methods for choroidal evaluation in VKH disease.^{14,15} However, the low resolution of contact B-mode ultrasonography and the anatomic alterations induced by the disease make visualization of the boundaries between the retina, the choroid, and the sclera difficult to discern.

Vogt-Koyanagi-Harada disease is usually treated with high-dose corticosteroids initially followed by a tapering oral dose.¹ Aggressive early treatment may prevent progression to the chronic recurrent stage.¹⁸ In addition, chronic anterior uveitis and persistent choroidal inflammation may lead to development of choroidal neovascularization.^{19,20} Thus, the evaluation of the treatment response is important in the therapy of VKH disease. Enhanced depth imaging OCT offers a method to directly visualize the choroid. The boundaries between the retina and the RPE and in turn between the RPE and the choroid are readily visible. However, if there is thickening of the choroid so that it is $>1,000\ \mu\text{m}$, visualization of the boundary between the choroid and the inner sclera may be difficult. The test still has diagnostic utility at this point because a choroidal thickness of $1,000\ \mu\text{m}$ is much greater than normal.¹⁷

In the current study, the left eye of Patient 4 showed the leakage from the optic nerve head during fluorescein angiography without serous retinal detachment. Because patchy filling delay and indistinct choroidal vessels were observed during indocyanine green angiography, meningismus with cerebrospinal fluid pleocytosis and the tinnitus were found, and because the fellow eye had a typical serous retinal detachment, we had diagnosed the papillitis type of VKH disease as being present in the left eye of Patient 4. However, it is possible that this case was seen earlier in the progression of disease before the development of a frank detachment. This case had choroidal thickening and might represent the precursor state to serous retinal detachment. These findings suggest that EDI-OCT could be used to evaluate various stages of VKH during follow-up by examining regions of the eye not otherwise visualized, such as the choroid, which appears to be primarily affected in VKH in the first place. In addition, because the papillitis type of VKH disease is sometimes misdiagnosed as optic neuritis,²¹ examination of the choroid using EDI-OCT might be useful in differential diagnosis.

This retrospective study had several weaknesses including a small sample size and short-term follow-up. This study would require a much larger number of patients than was examined in the present study because of known interactions between choroidal thickness and age and also refractive error. More patients and longer

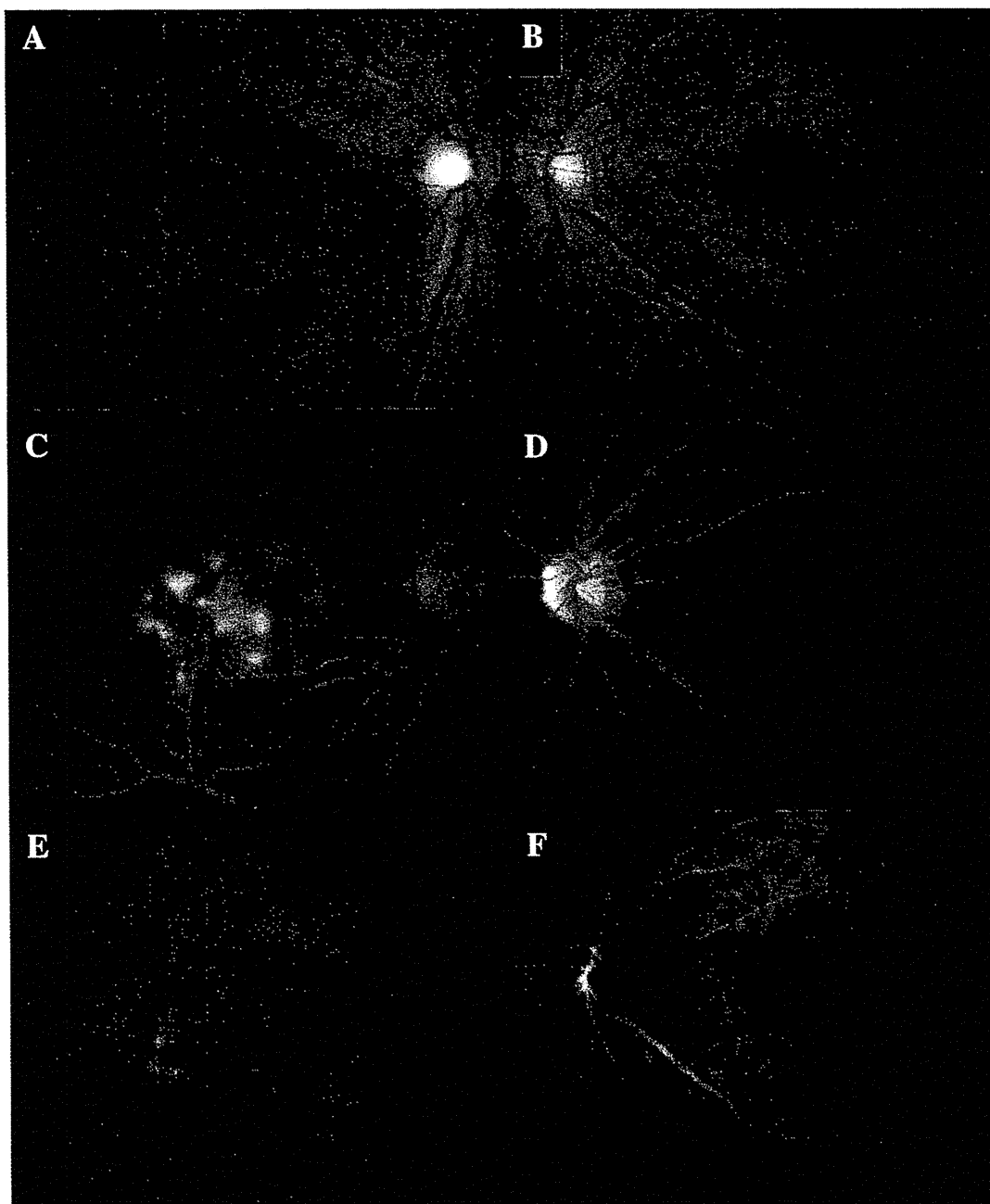


Fig. 4. Patient 4. A 17-year-old woman complained of decreased vision in the right eye for 2 days before presentation. The best-corrected visual acuity at baseline was 1.0 (20/20) (0.0 logMAR) in the right eye and 1.5 (20/13) (-0.18 logMAR) in the left eye. **A** and **B.** Monochromatic fundus photograph. At baseline, the right eye had a serous retinal detachment (**A**) and the left eye had foveal striate secondary to papillitis (**B**). **C** and **D.** Fluorescein angiography at baseline. **C.** Right eye showed multiple focal leaks and hyperfluorescence because of fluorescein pooling in the subretinal space. **D.** Left eye had fluorescein leakage from the optic disk. **E** and **F.** Indocyanine green angiography at baseline. Both eyes showed the multiple patchy filling delay with hypofluorescent spots and the indistinct choroidal vessels. She was diagnosed as having the ocular findings of VKH disease with serous retinal detachment in the right eye and papillitis in the left eye. She was given intravenous methylprednisolone (1000 mg, for 3 days) followed by tapered oral prednisolone starting at 40 mg/day.

follow-ups might provide the relationship among the choroidal thickness and the sign of the recurrence. In the current study, the acute stage of VKH disease showed marked choroidal thickening, which decreased dramatically after corticosteroid therapy. The serous retinal

detachment concomitantly disappeared with the decrease in choroidal thickness. As opposed to central serous chorioretinopathy, which has a thickened choroid¹⁸ and is adversely affected by corticosteroids, the excessive thickening in the choroid and the serous retinal

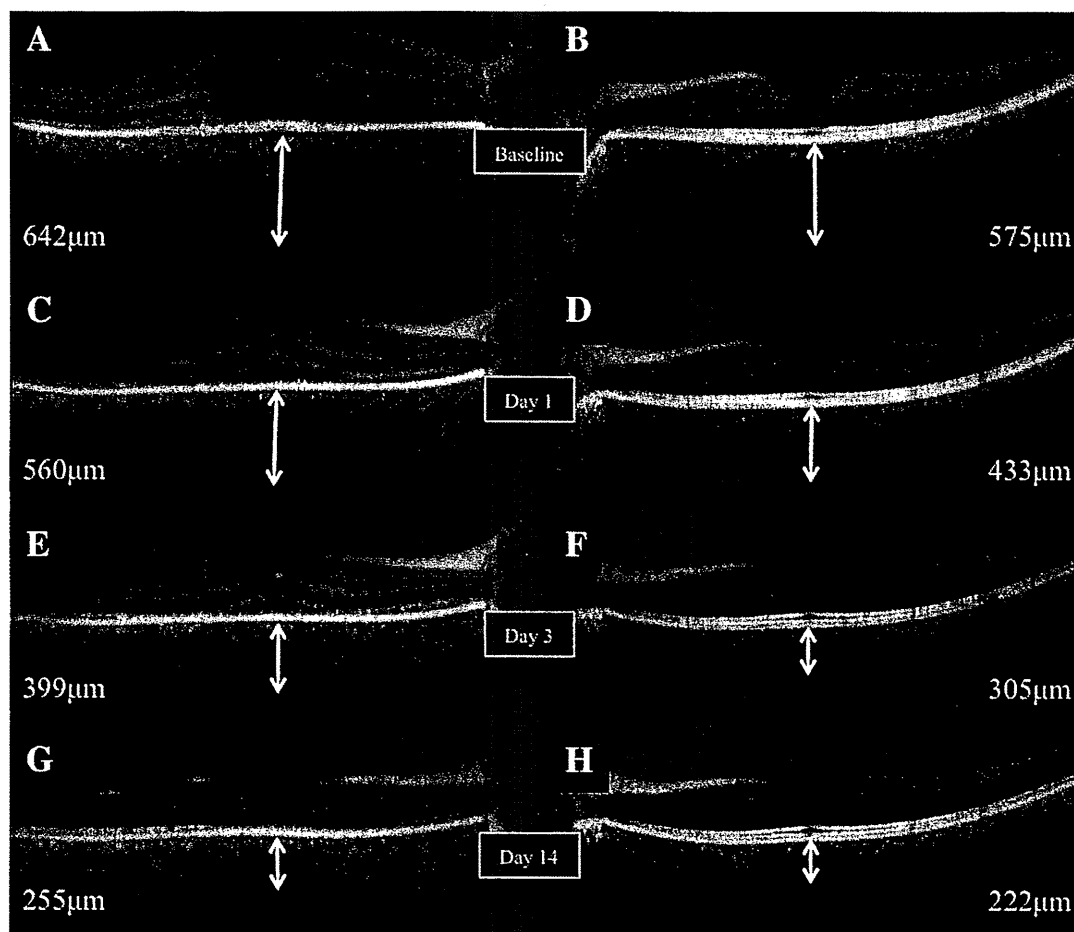


Fig. 5. Enhanced depth imaging spectral-domain OCT images of Patient 4. All images obtained using the technique described in this article were inverted. The right eye shows serous retinal detachment, and the left eye had no serous retinal detachment at baseline. The choroidal thickness from the horizontal scan was 642 μm in the right eye (A) and 575 μm in the left eye (B) at baseline, 560 μm in the right eye (C) and 433 μm in the left eye (D) at Day 1, 399 μm in the right eye (E) and 305 μm in the left eye (F) at Day 3, and 255 μm in the right eye (G) and 222 μm in the left eye (H) at Day 14. Resolution of the retinal detachment in the right eye was observed at Day 14. The best-corrected visual acuity on Day 14 was 1.2 (20/17) (-0.08 logMAR) in the right eye.

detachment in VKH are probably both primarily and secondarily related to inflammation, through increased vascular leakage. Enhanced depth imaging OCT is a very easy and useful adjunct to evaluate the choroidal involvement in VKH disease noninvasively.

Key words: Vogt–Koyanagi–Harada disease, enhanced depth imaging spectral-domain optical coherence tomography, choroidal thickness, retinal detachment, corticosteroid.

References

- Moorthy RS, Inomata H, Rao NA. Vogt-Koyanagi-Harada syndrome. *Surv Ophthalmol* 1995;39:265–292.
- Read RW, Holland GN, Rao NA, et al. Revised diagnostic criteria for Vogt-Koyanagi-Harada disease: report of an international committee on nomenclature. *Am J Ophthalmol* 2001;131:647–652.
- Okada AA, Mizusawa T, Sakai J, Usui M. Videofunduscopy and videoangiography using the scanning laser ophthalmoscope in Vogt-Koyanagi-Harada syndrome. *Br J Ophthalmol* 1998;82:1175–1181.
- Oshima Y, Harino S, Hara Y, Tano Y. Indocyanine green angiographic findings in Vogt-Koyanagi-Harada disease. *Am J Ophthalmol* 1996;122:58–66.
- Kohno T, Miki T, Shiraki K, et al. Subtraction ICG angiography in Harada's disease. *Br J Ophthalmol* 1999;83:822–833.
- Spaide RF, Goldbaum M, Wong DW, Tang KC, Iida T. Serous detachment of the retina. *Retina* 2003;23:820–846.
- Herbert CP, Mantovani A, Bouchenaki N. Indocyanine green angiography in Vogt-Koyanagi-Harada disease: angiographic signs and utility in patient follow-up. *Int Ophthalmol* 2007;27:173–182.
- Maruyama Y, Kishi S. Tomographic features of serous retinal detachment in Vogt-Koyanagi-Harada syndrome. *Ophthalmic Surg Lasers Imaging* 2004;35:239–242.
- Tsujikawa A, Yamashiro K, Yamamoto K, Nonaka A, Fujihara M, Kurimoto Y. Retinal cystoid spaces in acute Vogt-Koyanagi-Harada syndrome. *Am J Ophthalmol* 2005;139:670–677.
- Yamaguchi Y, Otani T, Kishi S. Tomographic features of serous retinal detachment with multilobular dye pooling in acute Vogt-Koyanagi-Harada disease. *Am J Ophthalmol* 2007;144:260–265.
- Gupta V, Gupta A, Gupta P, Sharma A. Spectral-domain cirrus optical coherence tomography of choroidal striations seen in the acute stage of Vogt-Koyanagi-Harada disease. *Am J Ophthalmol* 2009;147:148.e2–153.e2.

12. Shimizu K, Harada's, Behcet's, Vogt-Koyanagi syndromes— are they clinical entities? *Trans Am Acad Ophthalmol Otolaryngol* 1973;77:OP281–OP290.
13. Ohno S, Char DH, Kimura SJ, O'Connor GR. Vogt-Koyanagi-Harada syndrome. *Am J Ophthalmol* 1977;83:735–740.
14. Forster DJ, Cano MR, Green RL, Rao NA. Echographic features of the Vogt-Koyanagi-Harada syndrome. *Arch Ophthalmol* 1990;108:1421–1426.
15. Hewick SA, Fairhead AC, Culy JC, Atta HR. A comparison of 10 MHz and 20 MHz ultrasound probes in imaging the eye and orbit. *Br J Ophthalmol* 2004;88:551–555.
16. Spaide RF, Koizumi H, Pozonni MC. Enhanced depth imaging spectral-domain optical coherence tomography. *Am J Ophthalmol* 2008;146:496–500.
17. Margolis R, Spaide RF. A pilot study of enhanced depth imaging optical coherence tomography of the choroid in normal eyes. *Am J Ophthalmol* 2009;147:811–815.
18. Bykhovskaya I, Thorne JE, Kempen JH, Dunn JP, Jabs DA. Vogt-Koyanagi-Harada disease: clinical outcomes. *Am J Ophthalmol* 2005;140:674–678.
19. Moorthy RS, Chong LP, Smith RE, Rao NA. Subretinal neovascular membranes in Vogt-Koyanagi-Harada syndrome. *Am J Ophthalmol* 1993;116:164–170.
20. Read RW, Rechodouni A, Butani N, et al. Complications and prognostic factors in Vogt-Koyanagi-Harada disease. *Am J Ophthalmol* 2001;131:599–606.
21. Rajendram R, Evans M, Khurana RN, Tsai JH, Rao NA. Vogt-Koyanagi-Harada disease presenting as optic neuritis. *Int Ophthalmol* 2007;27:217–220.

Subfoveal Retinal and Choroidal Thickness After Verteporfin Photodynamic Therapy for Polypoidal Choroidal Vasculopathy

ICHIRO MARUKO, TOMOHIRO IIDA, YUKINORI SUGANO, MASAOKI SAITO, AND TETSUJU SEKIRYU

- **PURPOSE:** To evaluate the morphologic retinal and choroidal changes after verteporfin photodynamic therapy (PDT) with and without ranibizumab for polypoidal choroidal vasculopathy using spectral-domain optical coherence tomography.
- **DESIGN:** Retrospective, comparative series.
- **METHODS:** The enhanced depth imaging optical coherence tomography technique was used in this retrospective, comparative series to measure the subfoveal retinal and choroidal thicknesses before and after treatment.
- **RESULTS:** Twenty-seven eyes with polypoidal choroidal vasculopathy were examined retrospectively. Sixteen eyes were treated with PDT monotherapy (PDT group). Eleven eyes were treated with PDT after intravitreal ranibizumab injection (ranibizumab plus PDT group). The polypoidal lesions regressed in all cases at 3 months. The mean retinal thickness, including the retinal detachment, increased from $401 \pm 157 \mu\text{m}$ before treatment to $506 \pm 182 \mu\text{m}$ 2 days after PDT ($P < .001$) and decreased to $365 \pm 116 \mu\text{m}$ by 1 week after treatment ($P = .03$) and $265 \pm 127 \mu\text{m}$ by 6 months after treatment ($P < .001$). The mean choroidal thickness increased from $269 \pm 107 \mu\text{m}$ before treatment to $336 \pm 96 \mu\text{m}$ 2 days after PDT treatment ($P < .001$ compared with baseline) and decreased to $262 \pm 96 \mu\text{m}$ by 1 week after treatment ($P = .24$) and $229 \pm 104 \mu\text{m}$ by 6 months ($P < .001$). Although the choroidal thickness showed a similar trend with both therapies, the retinal thickness in the ranibizumab plus PDT group remained thinner than that in the PDT group until 6 months after treatment.
- **CONCLUSIONS:** PDT was associated with decreased retinal and choroidal thicknesses. Combination therapy reduced the transient exudation after PDT in some cases, and monthly intravitreal ranibizumab injections maintained retinal thinning and seemed to improve vision better than PDT monotherapy. (Am J Ophthalmol 2011;151:594–603. © 2011 by Elsevier Inc. All rights reserved.)

Accepted for publication Oct 20, 2010.

From the Department of Ophthalmology, Fukushima Medical University School of Medicine, Fukushima, Japan (I.M., T.I., Y.S., M.S., Y.S.).

Inquiries to Ichiro Maruko, Department of Ophthalmology, Fukushima Medical University School of Medicine, 1 Hikarigaoka, Fukushima, Japan; e-mail: imaruko@fmu.ac.jp

VERTEPORFIN PHOTODYNAMIC THERAPY (PDT), Visudine; Novartis, Basel, Switzerland) is an established treatment for age-related macular degeneration (AMD)^{1–5} and polypoidal choroidal vasculopathy (PCV).^{5–11} However, complications after PDT have been reported,^{12–24} such as transient subretinal or intraretinal fluid accumulation within 1 week after PDT and more severe and potential permanent vision loss secondary to subretinal bleeding. PDT using verteporfin for AMD also can cause choriocapillaris damage and vascular remodeling in the underlying choroid.^{12–15,23,24}

Intravitreal ranibizumab (Lucentis; Genentech, South San Francisco, California, USA), an anti-vascular endothelial growth factor (VEGF) therapy, is the most commonly used therapy for AMD,^{25–27} although the efficacy of anti-VEGF therapy for PCV may be less than that for typical choroidal neovascularization associated with AMD.^{28–30} Since PDT is thought to induce VEGF expression,¹⁹ combination therapy comprising PDT and pharmacologic agents^{29,31–34} to inhibit VEGF expression also has been reported to increase the efficacy of both PDT and pharmacologic agents.

Spectral-domain optical coherence tomography (OCT) detects morphologic changes in the neurosensory retina in a variety of retinal and choroidal diseases. Recently, Spaide and associates reported a new method, enhanced depth imaging (EDI) OCT, to evaluate the choroidal status.³⁵

In the current study, we retrospectively evaluated visual acuity (VA) changes and retinal and choroidal alterations after PDT for PCV using this noninvasive OCT technique. We also compared these changes after PDT with and without intravitreal injection of ranibizumab.

METHODS

THE CLINICAL EXAMINATIONS FOR DIAGNOSIS OF PCV INCLUDED indirect ophthalmoscopy, slit-lamp biomicroscopy with a contact lens or noncontact lens, digital fluorescein angiography, and indocyanine green angiography (ICGA). We used a digital imaging system with an infrared camera and standard fundus camera (TRC-50 IX/IMAGeNet H1024 system; Topcon, Tokyo, Japan) and a confocal laser scanning system (HRA-2; Heidelberg Engineering, Dos-

TABLE. The Clinical Changes of the Mean Choroidal Thickness and the Mean Retinal Thickness during the Follow-up Periods in the Photodynamic Therapy Alone Group and the Ranibizumab plus Photodynamic Therapy Group

Case No.	Gender	Age (yrs)	Eye	Treatment	BCVA at Baseline (logMAR)	BCVA at 6 Mos (logMAR)	Permeability ^a	Retinal Thickness (μm) ^b						Choroidal Thickness (μm) ^c							
								Baseline	Day 0	Day 2	1 Wk	1 Mo	3 Mos	6 Mos	Baseline	Day 0	Day 2	1 Wk	1 Mos	3 Mos	6 Mos
1	M	56	Left	PDT ^d	0.6 (0.22)	1.0 (0.00)	Yes	253	268	259	222	235	198	373	421	363	323	324	292		
2	M	77	Left	PDT	0.1 (1.00)	0.3 (0.52)	Yes	345	512	394	293	293	209	337	414	295	215	204	208		
3	M	58	Left	PDT	0.4 (0.40)	1.0 (0.00)	Yes	670	610	508	421	410	314	327	402	291	290	284	284		
4	M	62	Left	PDT	0.6 (0.22)	0.8 (0.10)	Yes	374	465	373	211	190	191	191	251	174	134	129	129		
5	M	86	Right	PDT	0.2 (0.70)	0.3 (0.52)	Yes	218	258	250	189	149	137	322	420	341	258	280	246		
6	M	76	Left	PDT	0.5 (0.30)	0.5 (0.30)	Yes	230	297	267	230	279	201	307	352	320	306	282	278		
7	M	69	Left	PDT	0.7 (0.15)	0.8 (0.10)	Yes	295	589	281	195	160	177	458	492	464	444	424	435		
8	M	70	Left	PDT	0.6 (0.22)	0.9 (0.05)	Yes	281	438	343	227	216	208	348	364	335	312	307	323		
9	F	76	Right	PDT	0.2 (0.70)	0.2 (0.70)	Yes	364	451	322	275	175	209	261	281	225	196	206	208		
10	F	70	Left	PDT	0.4 (0.40)	0.7 (0.15)	Yes	385	436	345	328	321	307	290	306	286	264	243	265		
11	M	82	Right	PDT	0.08 (1.10)	0.1 (1.00)	No	476	731	379	431	1037	681	250	266	228	216	191	146		
12	M	82	Right	PDT	0.3 (0.52)	NA	No	435	548	408	178	168	NA	127	253	146	117	107	NA		
13	M	86	Right	PDT	0.05 (1.30)	0.03 (1.52)	No	466	505	332	216	277	243	120	234	156	112	116	116		
14	M	53	Left	PDT	0.3 (0.52)	0.4 (0.40)	No	276	345	234	232	270	326	159	268	177	158	168	178		
15	F	68	Right	PDT	0.4 (0.40)	0.4 (0.40)	No	368	645	407	190	249	388	217	249	197	183	186	208		
16	F	77	Right	PDT	0.4 (0.40)	1.2 (-0.08)	No	387	405	338	215	161	174	292	328	312	241	215	213		
Mean ± SD		71.8			0.29 (0.53)	0.42 (0.37)		364	469	340	253	287	264	273	331	269	235	229	235		
17	M	55	Left	Ranibizumab + PDT ^e	0.5 (0.30)	0.8 (0.10)	Yes	348	313	305	257	190	179	276	604	595	645	510	508	505	508
18	M	78	Right	Ranibizumab + PDT	0.24 (0.62)	NA	Yes	542	535	951	516	406	330	NA	260	260	301	241	252	226	NA
19	F	67	Left	Ranibizumab + PDT	0.5 (0.30)	1.0 (0.00)	Yes	533	516	536	507	471	244	190	292	289	328	281	262	248	272
20	F	74	Left	Ranibizumab + PDT	0.5 (0.30)	0.8 (0.10)	Yes	213	207	544	186	128	150	174	344	351	425	371	311	323	383
21	F	72	Right	Ranibizumab + PDT	0.3 (0.52)	0.8 (0.10)	Yes	435	429	434	356	274	139	146	208	216	329	193	169	145	114
22	F	84	Right	Ranibizumab + PDT	0.01 (2.00)	0.04 (1.40)	Yes	955	853	1020	726	538	418	557	250	238	350	220	205	173	155
23	M	56	Right	Ranibizumab + PDT	0.3 (0.52)	0.4 (0.40)	No	324	328	312	246	221	213	228	248	248	273	229	198	224	245
24	M	67	Right	Ranibizumab + PDT	0.5 (0.30)	1.0 (0.00)	No	514	506	494	407	271	173	234	185	190	252	174	149	148	146
25	M	77	Left	Ranibizumab + PDT	0.3 (0.52)	0.8 (0.10)	No	476	464	506	394	230	181	188	224	229	401	273	205	164	176

Continued on next page

TABLE. Continued

Case No.	Gender	Age (yrs)	Eye	Treatment	BCVA at Baseline (logMAR)		Permeability ^f	Retinal Thickness (μm) ^b						Choroidal Thickness (μm) ^c							
					Baseline	BCVA at 6 Mos (logMAR)		Baseline	Day 0	Day 2	1 Wk	1 Mo	3 Mos	6 Mos	Baseline	Day 0	Day 2	1 Wk	1 Mos	3 Mos	6 Mos
26	M	67	Left	Ranibizumab + PDT	0.4 (0.40)	0.3 (0.52)	No	400	404	610	520	380	319	320	111	109	212	114	95	98	91
27	F	84	Right	Ranibizumab + PDT	0.5 (0.30)	0.6 (0.22)	No	268	284	444	300	246	388	360	175	165	253	169	158	150	117
Mean \pm		71.0			0.28 (0.55)	0.51 (0.29)		455	440	559	401	305	248	267	264	262	342	252	228	218	220
SD							198	173	230	157	127	99	122	129	127	119	109	110	113	134	

BCVA = best-corrected visual acuity; F = female; logMAR = logarithm of the minimal angle of resolution; M = male; Mos = months; NA = not applicable; PDT = photodynamic therapy; SD = standard deviation; Wk = week; yrs = years.

^aChoroidal vascular hyperpermeability.

^bChoroidal thickness measured using the enhanced depth imaging spectral-domain optical coherence tomography technique.

^cRetinal thickness including retinal detachment at the fovea.

^dRetinal thickness including retinal detachment at the fovea.

^ePhotodynamic therapy with verteporfin. In the PDT alone group, measurement was at the fovea before PDT (baseline), 2 days after PDT (day 2), 1 week after PDT (day 1W), 1 month after laser PDT (1M), 3 months after PDT (3M), and 6 months after PDT (6M).

^fIntravitreal ranibizumab injection plus PDT in the ranibizumab plus PDT group, measurement was at the fovea before ranibizumab (baseline), before PDT (day 0), 2 days after PDT (day 2), 1 week after PDT (1W), 1 month after PDT (1M), 3 months after PDT (3M), and 6 months after PDT (6M).

senheim, Germany). The best-corrected visual acuity (BCVA) was measured with a Japanese standard decimal visual chart and converted to the logarithm of the minimal angle of resolution (logMAR) scale for analysis. All eyes were examined with the Heidelberg Spectralis OCT (Heidelberg Engineering, Heidelberg, Germany).

In the current study, diagnostic criteria for PCV were proposed based on ICGA findings, which imaged the characteristic aneurysmal lesions. All patients with PCV had choroidal neovascularization on fluorescein angiography, which was identified as PCV on ICGA. Choroidal vascular hyperpermeability, seen as hyperfluorescence in middle-phase ICGA images, also was evaluated.

Consecutive patients with PCV were treated with PDT monotherapy (PDT group) between January 2009 and May 2009 and were treated with the combination therapy of intravitreal ranibizumab and PDT (ranibizumab plus PDT group) between June 2009 and October 2009. Ranibizumab became available for medical use in Japan in March 2009.

The patients in the ranibizumab plus PDT group were treated 1 or 2 days before PDT with intravitreal ranibizumab (0.5 mg/0.05 mL) injected 3.5 to 4.0 mm posterior to the corneal limbus into the vitreous cavity using a 30-gauge needle after topical anesthesia was applied. Consecutive monthly intravitreal ranibizumab injections were administered for 3 months.

PDT was performed in both groups using the standard dose (6 mg/m²) of verteporfin according to the protocol of the Treatment of Age-Related Macular Degeneration with Photodynamic Therapy studies,^{1,2} except for the greatest linear dimension (GLD). The GLD and treatment spot size were measured on ICGA (ICG-guided PDT) to reduce the exposed area.³⁶⁻³⁸ The diameter of the PDT treatment spot size was the GLD plus 1 mm. A 689-nm laser system (Carl Zeiss, Dublin, California, USA) was used, and 50 J/cm² of energy was delivered with an 83-second exposure time. Angiographic evaluation in all cases was examined at 3 months after PDT, and additional treatment was performed if needed.

The retinal thickness, defined as the distance between the inner surface of the neurosensory retina and the inner surface of the retinal pigment epithelium, including retinal detachments at the fovea, also was measured at the same time. Spaide and associates reported observing the morphologic choroidal changes using the EDI OCT technique, which obtained inverted and highlighted choroidal images by moving the OCT device close to the eye.³⁵ All images were obtained using an eye-tracking system, and 100 scans were averaged automatically to improve the signal-to-noise ratio. We measured the choroidal thickness, defined as the zonal area between the outer surface of the retinal pigment epithelium and the inner scleral surface, from vertical and horizontal sections under the center of the fovea from OCT data, and these were averaged.

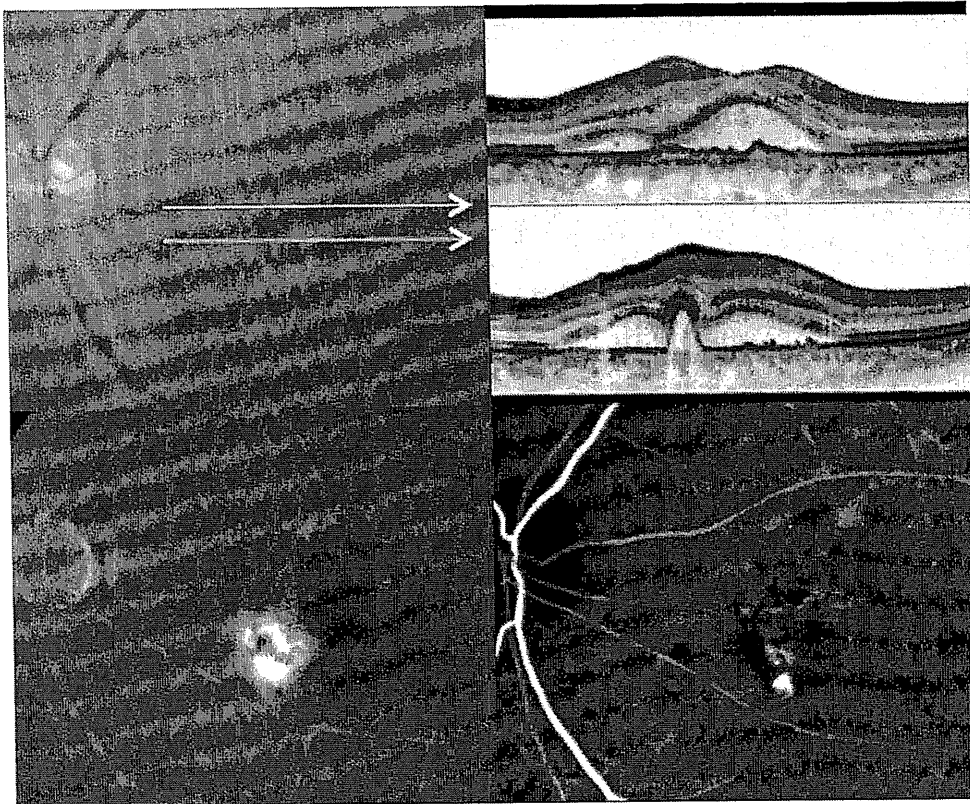


FIGURE 1. Case 4, a representative case from the photodynamic therapy group with polypoidal choroidal vasculopathy, is a 62-year-old man who sought treatment for decreased vision in the left eye 2 weeks previously. (Top left) Gray-scale fundus photograph of the left eye showing a serous retinal detachment at the center of the macular area and an elevated orange-red lesion at the lower area nasal to the fovea. The white horizontal arrows indicate the line through the fovea and orange-red lesions, respectively. (Top right) Spectral-domain optical coherence tomography images of the left eye showing the serous retinal detachment, retinal pigment epithelium irregularity, and a sharp protrusion. The upper and lower images correspond to the arrows on the gray-scale fundus photography, respectively. (Bottom left) Middle-phase fluorescein angiography image showing leakage in the lower area nasal to the fovea. (Bottom right) Middle-phase indocyanine green angiography image showing the polypoidal lesion and the abnormal vascular network at the macular area.

In the PDT group, the retinal and choroidal thicknesses at the center of the fovea were measured using the EDI OCT before PDT (baseline) and after PDT at 2 days, 1 week, and 1, 3, and 6 months. In the ranibizumab plus PDT group, the retinal and choroidal thicknesses at the center of the fovea also were measured by EDI OCT before intravitreal injection of ranibizumab (baseline), before PDT on day 1 or 2 after the intravitreal ranibizumab injection (day 0), and after PDT at 2 days, 1 week, and 1, 3, and 6 months. OCT was performed at all visits. The patients who received their first PDT treatments remained in the hospital for 2 days to avoid sun exposure.

The reported measurements obtained from the OCT images represented the average of all the measurements. The coauthors (I.M., Y.S., M.S.) were masked to the treatment status. The VAs are expressed as decimal equivalents and logMAR equivalents. The BCVA and the measurement of the choroidal and retinal thickness were analyzed using the Wilcoxon signed-rank test (SPSS soft-

ware version 17.0; SPSS, Inc, Chicago, Illinois, USA), and $P = .05$ or less was considered significant.

RESULTS

TWENTY-SEVEN EYES OF 27 CONSECUTIVE PATIENTS WITH newly diagnosed PCV were included. Sixteen eyes of 16 patients (12 men, 4 women; mean age, 71.8 years) comprised the PDT group. Eleven eyes of 11 patients (6 men, 5 women; mean age, 71.0 years) comprised the ranibizumab plus PDT group. The lesion area included the fovea in all cases. The mean GLD for PDT was $3013 \pm 1059 \mu\text{m}$ in the PDT group and $2905 \pm 1122 \mu\text{m}$ in the ranibizumab plus PDT group. ICGA showed that the polypoidal lesions in all cases in both groups regressed at 3 months. One eye in the ranibizumab plus PDT group needed retreatment; 3 eyes in the PDT group needed retreatment for the exuda-

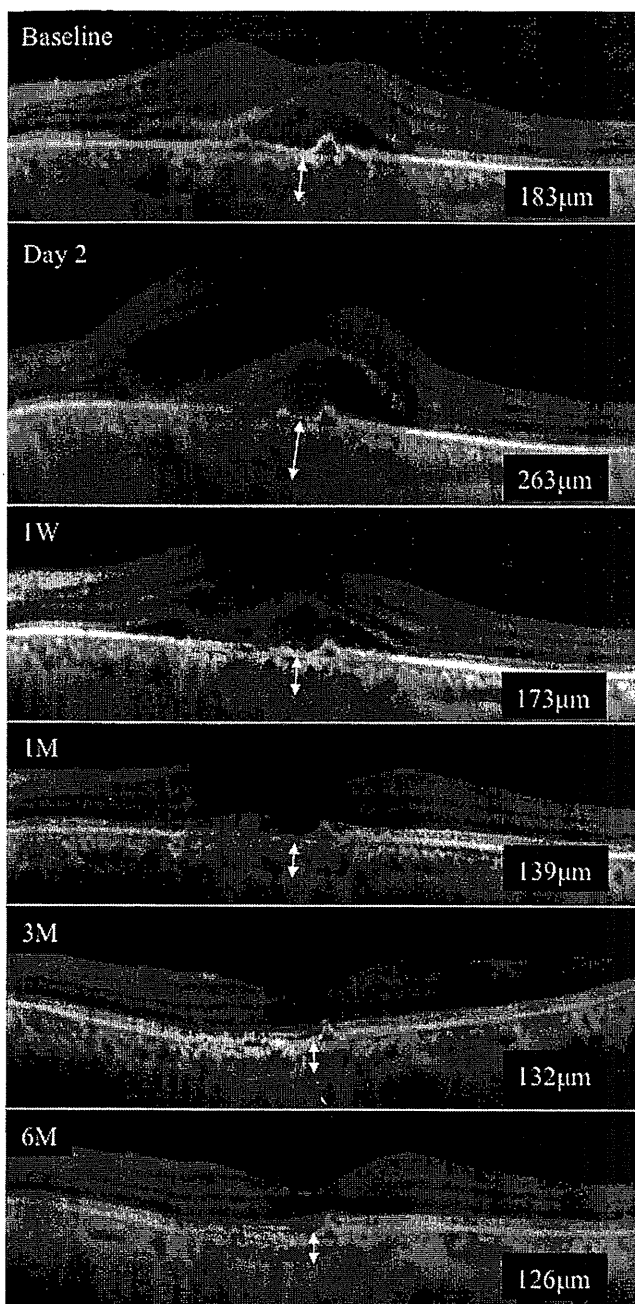


FIGURE 2. Enhanced depth imaging spectral-domain optical coherence tomography images of the same polypoidal choroidal vasculopathy case as in Figure 1. The choroidal thickness in the horizontal images at baseline (Top) was 183 μm , (Second row) increased markedly to 263 μm on day 2, (Third row) decreased to 173 μm at 1 week, (Fourth row) decreased to 139 μm at 1 month, (Fifth row) decreased to 132 μm at 3 months, and (bottom) decreased to 126 μm at 6 months. The serous retinal detachment resolved in 3 months. Baseline = before photodynamic therapy (PDT); day 2 = 2 days after PDT; 1 W = 1 week after PDT; 1 M = 1 month after PDT; 3 M = 3 months after PDT; 6 M = 6 months after PDT.

tive findings during the follow-up period. One patient in each group did not return for the 6-month visit.

The mean retinal thickness increased significantly ($P < .001$) from $401 \pm 157 \mu\text{m}$ at baseline to $506 \pm 182 \mu\text{m}$ on day 2 after PDT and decreased to $365 \pm 116 \mu\text{m}$ by 1 week ($P = .03$), $274 \pm 102 \mu\text{m}$ by 1 month ($P < .001$), $271 \pm 174 \mu\text{m}$ by 3 months ($P < .001$), and $265 \pm 127 \mu\text{m}$ by 6 months ($P < .001$). The mean choroidal thickness increased from $269 \pm 107 \mu\text{m}$ at baseline to $336 \pm 96 \mu\text{m}$ on day 2 after PDT ($P < .001$) and decreased to $262 \pm 96 \mu\text{m}$ by 1 week ($P = .24$), $232 \pm 96 \mu\text{m}$ by 1 month ($P < .001$), $225 \pm 95 \mu\text{m}$ by 3 months ($P < .001$), and $229 \pm 104 \mu\text{m}$ by 6 months ($P < .001$). The mean choroidal thickness of 16 eyes with choroidal vascular hyperpermeability in middle-phase baseline ICGA images was thicker than in 11 eyes without hyperpermeability ($323 \pm 99 \mu\text{m}$ vs $191 \pm 60 \mu\text{m}$; $P < .001$, Mann-Whitney U test).

The mean subfoveal retinal and choroidal thicknesses at baseline and the changes during follow-up in both groups are summarized in the Table. Figures 1 and 2 show representative cases in the PDT group. Figures 3 and 4 show representative cases in the ranibizumab plus PDT group.

In the PDT group, the mean choroidal thickness increased from $273 \pm 93 \mu\text{m}$ at baseline to $331 \pm 80 \mu\text{m}$ on day 2 ($P < .001$) and decreased to $269 \pm 88 \mu\text{m}$ by 1 week ($P = .5$), $229 \pm 85 \mu\text{m}$ by 3 months ($P < .001$), and $235 \pm 83 \mu\text{m}$ by 6 months ($P < .001$). In the ranibizumab plus PDT group, the mean choroidal thickness increased from $264 \pm 129 \mu\text{m}$ at baseline to $342 \pm 119 \mu\text{m}$ on day 2 after PDT ($P = .003$) and decreased to $252 \pm 109 \mu\text{m}$ by 1 week ($P = .21$), $218 \pm 113 \mu\text{m}$ by 3 months ($P = .003$), and $220 \pm 134 \mu\text{m}$ by 6 months ($P = .001$). The changes in the choroidal thicknesses in both groups were similar. The changes in the mean retinal thickness also showed a similar trend toward decreased thickness over 6 months. Although the mean retinal thickness in the PDT group increased significantly from $364 \pm 114 \mu\text{m}$ at baseline to $469 \pm 137 \mu\text{m}$ on day 2 after PDT ($P = .003$), that in the ranibizumab plus PDT group did not increase significantly on day 2 after PDT ($455 \pm 198 \mu\text{m}$ at baseline, $559 \pm 230 \mu\text{m}$ on day 2; $P = .09$). Only 1 eye in the PDT group had retinal thinning on day 2 after PDT; however, 5 eyes in the ranibizumab plus PDT group had retinal thinning.

The changing ratios of the retinal and choroidal thicknesses compared with baseline in both groups are shown in Figure 5. Both graphs showed a similar curve after PDT; however, the percentage change of the retinal thickness at 6 months was 73% in the PDT group and 59% in the ranibizumab plus PDT group. The retinal thickness at 6 months remained relatively lower in the ranibizumab plus PDT group than in the PDT group.

The mean BCVA levels in all cases at baseline and at 1, 3, and 6 months were 0.29 (0.54 logMAR), 0.37 (0.43 logMAR), 0.42 (0.38 logMAR), and 0.46 (0.34 logMAR),

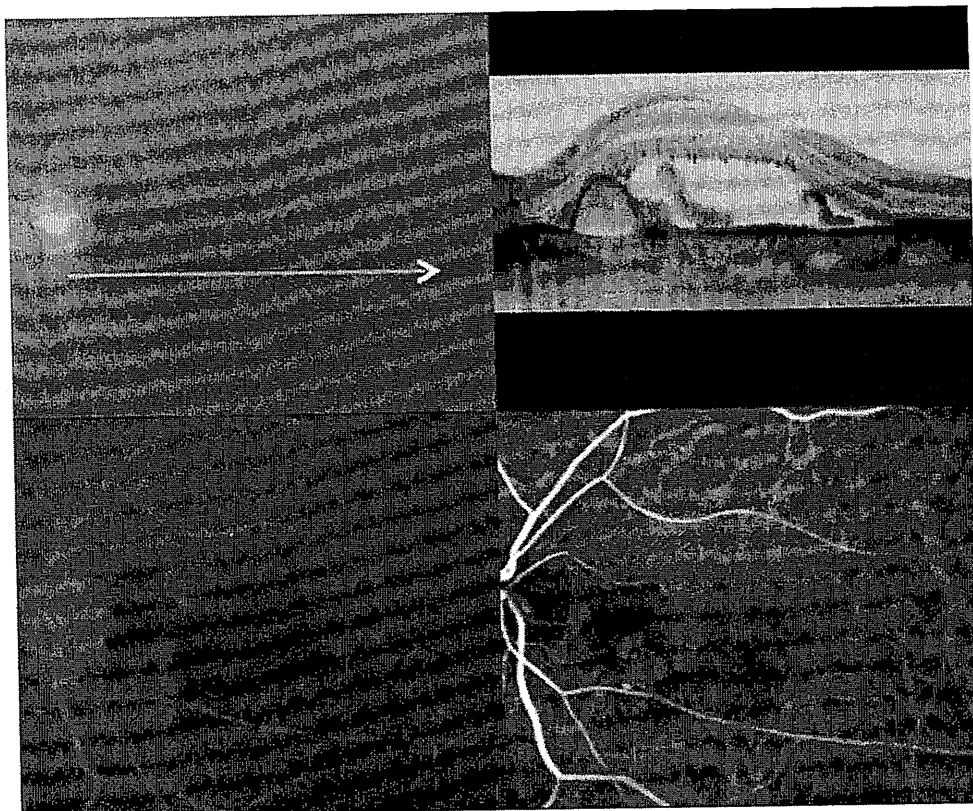


FIGURE 3. Case 25, a representative case of polypoidal choroidal vasculopathy in the ranibizumab-photodynamic therapy group, is a 77-year-old man who noted blurred vision in the left eye 2 weeks previously. (Top left) Gray-scale fundus photograph of the left eye showing a serous retinal detachment at the macular area and a subretinal hemorrhage between the optic disc and fovea. The white horizontal arrows indicate the line through the fovea. (Top right) Spectral-domain optical coherence tomography image of the left eye showing the serous retinal detachment at the macular area and a sharp protrusion temporal to the optic disc. The image corresponds to the arrows of the gray-scale fundus photograph. (Bottom left) Middle-phase fluorescein angiography image showing slight leakage at the lower area nasal to the fovea. (Bottom right) Middle-phase indocyanine green angiography image showing a polypoidal lesion and the abnormal vascular network at the lower-nasal area to the fovea.

respectively. There was a significant ($P < .001$) improvement from baseline to 6 months. The mean BCVA levels in the PDT group at the same time points were 0.29 (0.53 logMAR), 0.37 (0.43 logMAR), 0.37 (0.43 logMAR), and 0.42 (0.37 logMAR), respectively. The mean BCVA levels in the ranibizumab plus PDT group at the same time points were 0.28 (0.55 logMAR), 0.38 (0.42 logMAR), 0.49 (0.31 logMAR), and 0.51 (0.29 logMAR), respectively. Although both groups had significant improvements in VA compared with baseline ($P = .01$ in both groups), the BCVA in the ranibizumab plus PDT group was better than that in the PDT group (Figure 6).

DISCUSSION

IN THE CURRENT STUDY, PDT OCCLUDED THE POLYPOIDAL lesions and decreased the retinal and choroidal thicknesses in eyes with PCV. The combination therapy of ranibizumab and PDT reduced the exudation just after

PDT and maintained the retinal thinning until 6 months after treatment. Consequently, the BCVA after combination therapy was relatively better than that after PDT monotherapy.

PCV is more common in Asia than in white persons^{39,40} and is thought to account for approximately half of patients with neovascular AMD in Japan.⁴¹ PDT for PCV is still an effective treatment in Japan because PDT may result in regression of polypoidal lesions.^{5,9-11} Currently, intravitreal ranibizumab is the most common treatment for AMD worldwide because of the expected increase in BCVA.²⁴⁻²⁶ However, there are increasing medical care costs and more regular hospital visits because of the need for monthly injections.^{42,43} In addition, intravitreal ranibizumab for PCV is less effective than for AMD.²⁸⁻³⁰

Although transient exudation was seen within 1 week after PDT in the current study, the subfoveal choroidal thickness after PDT in both groups decreased at 6 months. ICGA in eyes with PCV sometimes shows choroidal vascular hyperpermeability,⁴⁴ which was observed in 16

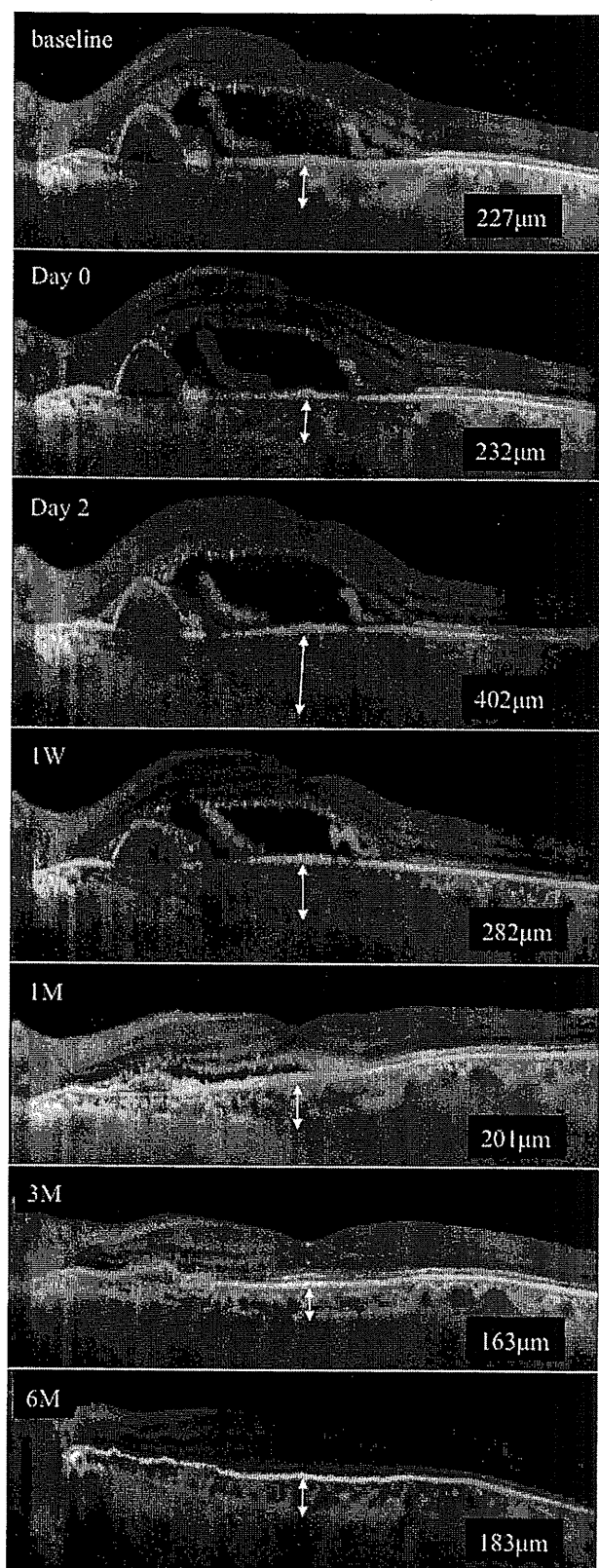


FIGURE 4. Enhanced depth imaging spectral-domain optical coherence tomography images in the same case of polypoidal choroidal vasculopathy as in Figure 3. The choroidal thicknesses in the horizontal images (Top) were 227 μm at baseline,

eyes in the current study. In patients with central serous chorioretinopathy (CSC), the choroid is thicker because of choroidal vascular hyperpermeability.⁴⁵ Serous retinal detachments develop more often than in typical AMD,⁴⁶ which may indicate that some cases of PCV are similar to central serous chorioretinopathy with a thickened choroid. In the current study, the choroid in eyes with choroidal vascular hyperpermeability was thicker than in eyes without hyperpermeability. All 10 eyes with hyperpermeability had retinal thinning at 6 months; however, 3 of 6 eyes without hyperpermeability had increased retinal thickness at 6 months in the PDT group. These findings may indicate that the activity of PCV could be evaluated by choroidal hyperpermeability. We previously reported that half-dose PDT in patients with chronic central serous chorioretinopathy reduced the choroidal thickness and caused serous retinal detachments to regress on EDI OCT.⁴⁷ These findings may suggest that the efficacy of PDT for PCV is associated with not only regression of polypoidal lesions, but also with reduced choroidal vascular hyperpermeability.

Combination therapy has been expected to require frequent intravitreal injections to enhance treatment efficacy.^{29,31-34} Some studies have reported that pharmacology-assisted PDT can reduce choriocapillaris occlusion.^{24,33}

In the current study, although the same trends in choroidal thickness in both treatment groups were observed after treatment, combination therapy compared with PDT monotherapy inhibited the temporary increase in retinal thickness in some cases and maintained the retinal thinning until 6 months of follow-up. Inhibition of the transient reaction after PDT in the ranibizumab plus PDT group was expected because of the transient induction of VEGF expression.¹⁹ Combination therapy significantly reduced the temporary exudation just after PDT; however, transient retinal thickening occurred in some cases. It is possible to inhibit the temporary inflammation using, for example, a steroid. Even with uncontrolled transient exudation after PDT, 3 consecutive monthly intravitreal ranibizumab injections may maintain the retinal thinning at 6 months and may help improve the VA. One patient had a recurrence after combination therapy, whereas 3 cases had a recurrence after PDT monotherapy during the follow-up period, which may indicate that ranibizumab also prevents fluid

(Second row) were 232 μm on day 0, (Third row) increased markedly to 402 μm on day 2, (Fourth row) decreased to 282 μm at 1 week, (Fifth row) decreased to 201 μm at 1 month, (Sixth row) decreased to 163 μm at 3 months, and (Bottom) increased to 183 μm at 6 months after treatment. The serous retinal detachment resolved at 3 months. Baseline = before intravitreal ranibizumab; day 0 = before photodynamic therapy (PDT); day 2 = 2 days after PDT; 1 W = 1 week after PDT; 1 M = 1 month after PDT; 3 M = 3 months after PDT; 6 M = 6 months after PDT.